Progress in Organic Coatings 139 (2020) 105325

Contents lists available at ScienceDirect

Progress in Organic Coatings

journal homepage: www.elsevier.com/locate/porgcoat

Crosslinking process, mechanical and antibacterial properties of UV-curable acrylate/Fe_3O_4-Ag nanocomposite coating

Thien Vuong Nguyen[a,b,*], Truc Vy Do[a], Manh Hung Ha[c], Hai Khoa Le[b], The Tam Le[a,d], Thi Ngoc Linh Nguyen[a,e], Xuan Thang Dam[f], Le Trong Lu[a,b], Dai Lam Tran[a,b], Quoc Trung Vu[g], Duc Anh Dinh[h], Tran Chien Dang[i], Phuong Nguyen -Tri[j]

[a] Graduate University of Science and Technology, VAST, 18 Hoang Quoc Viet, Cau Giay, Hanoi, Viet Nam
[b] Institute for Tropical Technology, VAST, 18 Hoang Quoc Viet, Cau Giay, Hanoi, Viet Nam
[c] Faculty of General Education, Hanoi University of Mining and Geology, Duc Thang, Bac Tu Liem, Hanoi, Viet Nam
[d] Vinh University, 182 Le Duan, Vinh, Nghe An, Viet Nam
[e] Thai Nguyen University of Sciences, Tan Thinh Ward, Thai Nguyen City, Viet Nam
[f] Faculty of Chemical Technology, Hanoi University of Industry, 298, Cau Dien, Bac Tu Liem, Hanoi, Viet Nam
[g] Faculty of Chemistry, Hanoi National University of Education, 136 Xuan Thuy, Cau Giay, Hanoi, Viet Nam
[h] NTT Hi-Tech Institute, Nguyen Tat Thanh University, 300A Nguyen Tat Thanh road, Ward 13, District 4, Ho Chi Minh City, Viet Nam
[i] Institute of Theorical and Applied Research (ITAR), Duy Tan University, Hanoi, 100000, Viet Nam
[j] Department of Chemistry, Biochemistry and Physic, Université du Québec à Trois-Rivieres, QC, Canada

ARTICLE INFO

Keywords:
Fe_3O_4-Ag nanohybrids
UV curing nanocomposite
Antimicrobial activity

ABSTRACT

In this paper, an antibacterial nanocomposite coating has been prepared by a green method based on photocroslinking with the addition of new synthesized Fe_3O_4-Ag nanohybrids. Fe_3O_4-Ag hybrid nanoparticles (0.1 wt. %) were dispersed in UV-curable acrylate resin stystem (BGDM and HDDA). The kinetic of UV-curing reaction of the nanocomposite was studited by measuring the coversion of acrylate double bonds, the variation of relative hardness, gel fraction and swelling degree of the coating. The structural morphology, mechanical and antibacterial properties of the nanocomposite were characterized. The analysis data demonstrated that the addition of 0.1 wt.% of Fe_3O_4-Ag hybrid nanoparticles into the coating affected insignificantly to its crosslinking process; the UV-exposure time to achieve a full crosslinking coating was about 4.8 s; the hybrid nanoparticles were homogeneously dispersed in network polymer matrix. The addition of the nanohybrids into the UV curing coating improved its its abrasion resistance from 98.24 to 126.54 lite/mil. The antibacterial testing indicated that the antimicrobial activity of the nanocomposite against *E. coli* was inversely proportional to its crosslinking density. Adding the nanocomposite in the culture, the growth rate of culture reduced about 3–5 % compared to that of the pure culture, after 5 h of cultivation while no antibacterial activity was observed for the neat coating.

1. Introduction

Organic coating is one of the most popular protection and decoration materials for different substrates [1,2]. To reduce the pollutants released into the atmosphere, in recent decades, non-solvent systems such as water-based and photocurable resin coatings have been developed [2–6]. Photocuring technology is a powerful technique for a wide range of applications. It has many oustanding properties, including transparency, high gloss, good mechanical properties as well as superior moisture, chemical and weathering resistance [4,7]. The UV-curing coating is formed by the photocrosslinking polymerization process of resins consisting of the main components: 1) photoinitiator; 2) multifunctional monomers or/and oligomers. There are two main types of photocurable resin systems: (1) radical photo-polymerization and (2) cationic photo-polymerization resin systems. The polymerization process usually undergoes four stages: photolysis of initiator, initiation, chain propagation and termination [7]. Antibacterial coating has been taken great of interests in research and development, especially, for tropical climate countries where bacterial and fungus grow strongly on the surface of different materials (woods, glass windows and walls). The application of antibacterial coating to protect against bacteria and fungi is essential.

In recent years, the addition of inorganic nanoparticles (such as TiO_2, ZnO and Ag) as antibacterial additives into paint formulation is a

* Corresponding author at: Institute for Tropical Technology, VAST, 18 Hoang Quoc Viet, Cau Giay, Hanoi, Viet Nam.
E-mail address: vuongvast@gmail.com (T.V. Nguyen).

https://doi.org/10.1016/j.porgcoat.2019.105325
Received 11 July 2019; Received in revised form 8 August 2019; Accepted 10 September 2019
Available online 04 December 2019
0300-9440/

major trend to make new antibacterial coatings [8–13]. In particular, Ag nanoparticles are the most effective solution as they exhibit high anti-microbial ability for both *Gram-positive* bacteria and *Gram-negative*. To enhance the antibacterial effect of Ag nanoparticles, Agparticles are often mounted on nanoscale metal oxides (for example, Fe_3O_4 or MnO_2 nanoparticles) [14–17]. In our previous papers, it was found that the Fe_3O_4–Ag hybrid nanoparticles had a better anti-microbial activity than that of the free Ag nanoparticles due to (1) the faster release of Ag^+ from the nanohybrids and (2) the accelerated ionization of Ag nanoparticles by Fe^{3+} ions [15–17]. The nanohybrids absorbed the light radiation in both UV and visible light ranges [15].

Althought, there are some literatures on the dispersion of different nanofillers in the UV-curable resins [12,18–22]. However, according to the best of our knowledge, at the moment, there is not any published works regarding photocurable Fe_3O_4-Ag nanohybrids reinforced coatings. In addition, it is known that crosslinking of thermoset resin system can be influenced by the nature and content of componnents as well as the present of additives [23–33]. In the case of epoxy matrix, Fe_3O_4 nanoparticles could play a role as a bridge interconnecting molecule, and thus reduced total free volume and increased the cross-linking density [24,25]. In this direction, to study the cure kinetics of epoxy/amine system, Fe_3O_4 nanoparticles were used as nanocarriers for loading of acid functional group [26], amine functional group [27,28], or hydroxyl functional group [27,29]. It was reported that the reaction of acid functional groups with amine groups of curing agent could possibly deactivated hardener [26]. Whereas, the presence of hydroxyl and amine groups might access to epoxy groups leading to increase in the amount of thermal curing [27]. Anti-corrosion and flame retardancy properties of nano-Fe_3O_4/epoxy nanocomposites were also viewed from Crosslinking intensity perspective [30]. For UV curable systems, effect of some additives on the photocrosslinking process has also been investigated. X. Allonas et al. have successfully synthesized organozirconiums from zirconium and organic fluorides and used them as the peroxyl radical scavengers against oxygen inhibition [32]. In the case of UV curing acrylic urethane coating, loading of 2 wt.% of Tinuvin 384 organic UV absorber was found to decrease the conversion of acrylate double bonds while A-TiO_2 and ZnO enhanced their conversion [33]. However, the role of Fe_3O_4-Ag nanohybrids as UV absorbed nanofillers in the curing reaction of the system has not been clarified.

In the current work, we quantitatively studied the crosslinking reaction of UV-curable systems based on acrylate resin and Fe_3O_4-Ag nanohybrids by spectroscopic analysis combined with monitoring the evolation of relative hardness and gel fraction of the coating. We also analyzed the morphology, mechanical properties and the influence of crossliking density of nanocomposite on the antimicrobial activity.

2. Materials and methods

2.1. Materials

2.1.1. Chemicals for the synthesis of Fe_3O_4–Ag nanhybrids

Iron (III) acetylacetonate ($Fe(acac)_3$, 99.99 %), silver nitrate (99.8 %), oleic acid (OA, 99 %), oleylamine (OLA, 70 %), 1-octadecanol (OCD-ol, 99 %), 1-octadecene (ODE, 90 %), absolute ethanol (100 %) and hexane (98.5 %) were purchased from Sigma-Aldrich Ltd, Singapore. All the materials were used as received without further purification.

2.1.2. UV-curable resin systems

1-Hydroxy-cyclohexyl-phenyl-ketone, Irgacure 184 (I.184) used as a photoinitiator was purchased from CIBA, Germany. 1,6-Hecxanediol diacrylate (HDDA, 80 %) used as a diluent and Bisphenol A glycerolate dimethacrylate (BGDM) were purchased from Sigma-Aldrich. Chemical structures of UV-curable compounds were presented in Fig. 1.

2.2. Sample preparation

2.2.1. Preparation of Fe_3O_4–Ag nanohybrids

Fe_3O_4–Ag nanohybrids were prepared following our previous work [17]. Fe_3O_4 nanoparticles are firstly pre-synthesized by thermal decomposition in an organic solvent of 1-octadecene [34]. The as-prepared Fe_3O_4 nanoparticles with the size of 8 nm were then used as seeds for the growing of Ag nanoparticles. Oleic acid and oleylamine act as surfactants to protect against agglomerations of nanoparticles. The reaction process of formation of Fe_3O_4–Ag hybrid nanoparticles can be described in Fig. 2.

Fig. 3 shows a photograph of solution of Fe_3O_4-Ag nanohybrids in n-hexane (Fig. 3a), their TEM image (Fig. 3b) and their schematic illustration of the morphology (Fig. 3c). As can be seen from these figures, the solution of Fe_3O_4-Ag nanohybrids shows a dark brown color; while the nanohybrids demonstrate a monodisperse and dumbbell-like structure. Ag nanoparticles have dimension of about 16 nm and Fe_3O_4 had dimension of about 8 nm as our recently reported. The presence of OA and OLA molecules on the surface of Fe_3O_4-Ag nanohybrids was determined by TGA measurement (Fig. 3d). A weight loss of 10.36 % in the temperature range of 70–550 °C was observed, which is assigned to the loss of residual 1-octadecanol and 1-octadecene solvents and water absorption on the particle surface during storage of samples (4.54 %) and the decomposition of OA/OLA surfactants (5.82 %).

2.2.2. Preparation of nanocomposite coating

A low content of nanoparticles (0.1 wt%) has been added to nanocomposites is because at high concentration, Fe_3O_4-Ag nanohybrids can cause UV shielding effect that can interfere with the UV-curing reaction. Moreover, for comparison reason with the antimicrobial activity of polyurethane acrylic coating [17], only 0.1 % content of nanoparticules is added. Fe_3O_4-Ag nanohybrids were firstly dispersed in HDDA by using a TPC-25 supersonic bath (Switzerland) for 3 h, they were then mixed with acrylate resin (BGDM) and photoinitiator (I.184) using an Ika RW16 Basic Mixer (England) for 0.5 h. the BGDM/HDDA/I.184 ratio is 55/45/3.

Coatings with thickness of ~ 25 μm were prepared either on KBr sheets for IR analysis, on Teflon sheets or on glass plates with the size of 100 × 100 × 2 mm for the measurements gel fraction and swelling and analyses of relative hardness, abrasion resistance and antibacterial activity using a spiral film applicator (Erichsen model 358). After that, the coatings were exposed to UV radiation of a medium-pressure mercury lamp (250 mW/cm^2) at room temperature, in the presence of air in FUSION UV equipment (Model F300S, USA). They were passed several times under the light with a web rate between 5 and 40 m/s and the exposure time is thus calculated. For example, for web rate of 40 m/s, exposure time is calculated, was 0.15 s. Fig. 4 presents photograph of neat coating and its nanocomposite containing 0.1 wt.% Fe3O4-Ag nanohybrids on glass sheets.

2.3. Characterization

2.3.1. Infrared spectroscopy analysis

The chemical conversion of acrylate double bonds band at 910 cm^{-1} (=CH stretching) during crosslinking was quantitatively investigated by using a FTIR spectrocoppy NEXUS 670 (Nicolet). Experiments are carried out at the same position of each sample before and after various UV exposures. To eliminate the effect of changes in coating thickness, cacbonyl band at 1730 cm^{-1} was chosen as the reference band.

The optical density (D) of groups was determinated by the following formula:

$$D = \varepsilon.l.C = \log (I_0/I) = \log [1 + H/(100\text{-}U)]$$

The relationship between I_0 and I with H and U was showed in Fig. 5 where H and U were calculated by using the software of FTIR

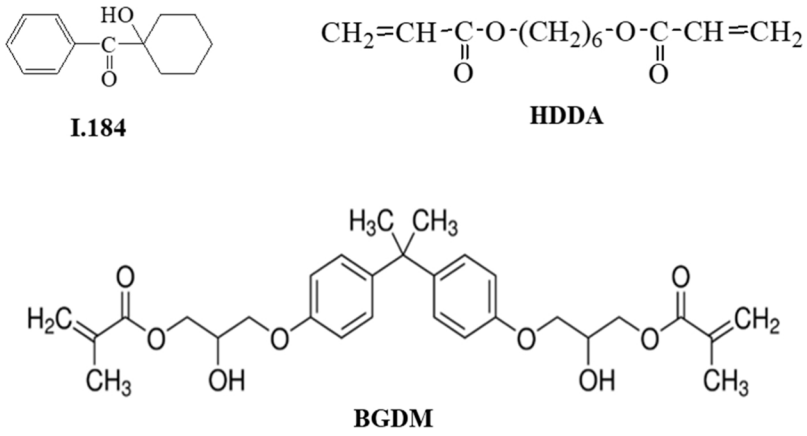

Fig. 1. Chemical formula of photoinitiator (I.184), diluent (HDDA) and acrylate resin (BGDM).

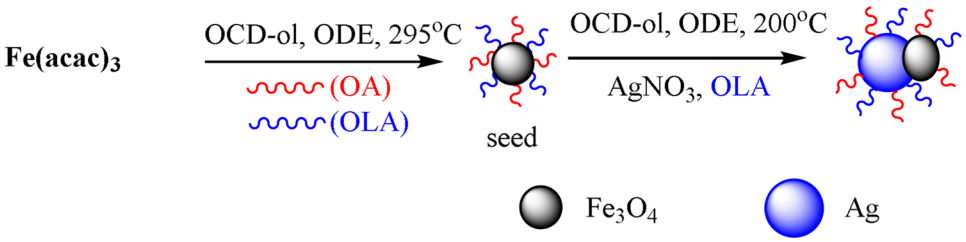

Fig. 2. The synthesis steps of Fe_3O_4–Ag hybrid nanoparticles.

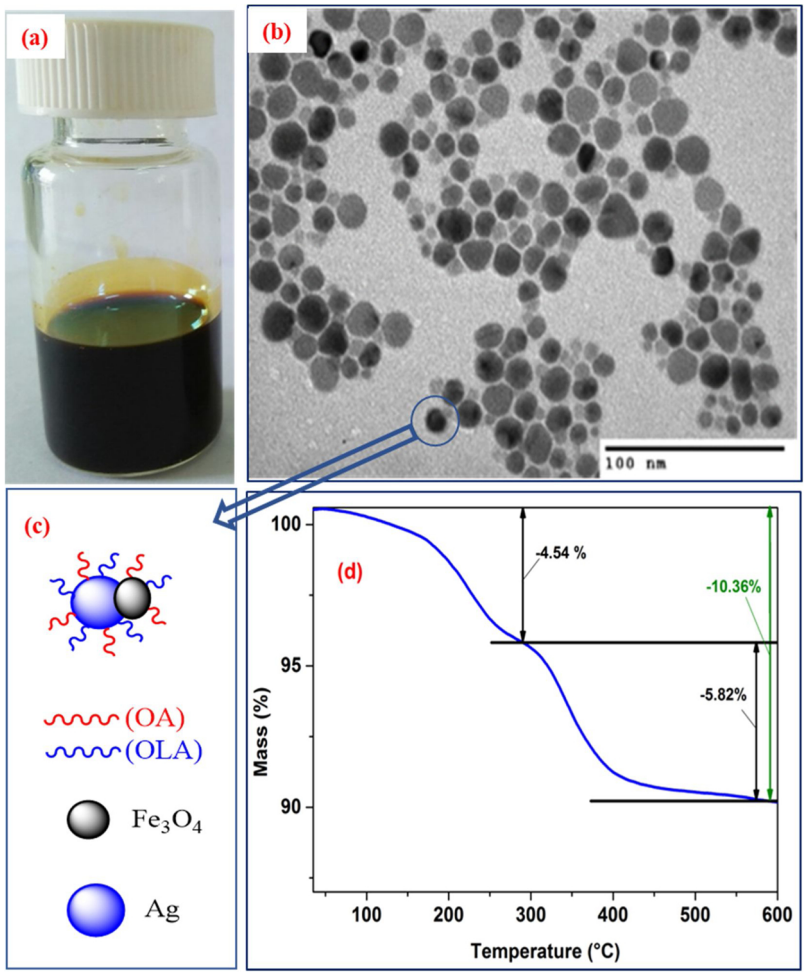

Fig. 3. Photograph of solution of OA/OLA coated Fe_3O_4-Ag nanohybrids in n-hexane (a), their TEM image (b), their structural morphology (c) and TGA scan (d).

Fig. 4. Photograph of neat coating (ACUV) and its nanocomposite containing 0.1 wt.% Fe3O4-Ag nanohybrids (ACUV/Fe_3O_4-Ag) on glass sheets.

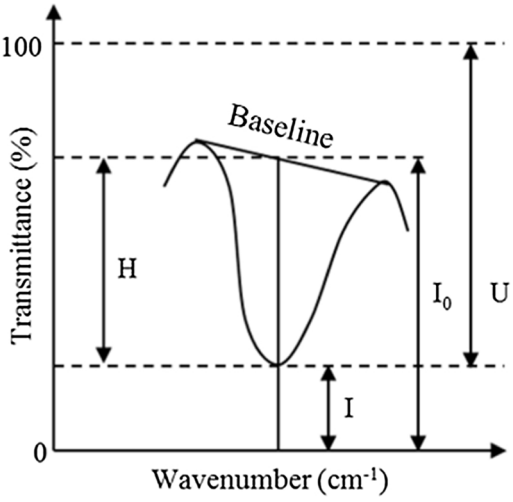

Fig. 5. The relationship between I_0 and I with H and U.

spectroscopy.

Remaining acrylate group was calculated as follows:

$$\text{Remaining acrylate group (\%)} = (D_{910\ cm\text{-}1}/D_{1730\ cm\text{-}1}) \times 100$$

2.3.2. Determination of gel fraction and swelling behavior

The swelling degree of cured coating samples was carried out in a Soxhlet in accordance with the standard ASTM D 2765 in acetone for 24 h to ananlyze the gel fraction and swelling degree of the coatings [17]. The insoluble film part was dried at 50 °C. The gel fraction is the weight of the insoluble film/the weight of the initial sample. The swelling degree is the weight of swollen film/the weight of dried film.

2.3.3. Measurement of mechanical properties

A Pendulum Damping Tester (model 300), in accordance with the Persoz Standard (NF T 30-016) was used to evaluate the relative hardness of the crosslinked coatings. The relative hardness of the coating is its absolute hardness/425. Abrasion resistance of the coatings was measured by using the abrasive falling methods, in according to the standard ASTM D968. All samples were determined triplicate and the data was presented as average values.

2.3.4. Morphology analysis of nanohybrids and nanocomposite

A Transmission Electron Microscopy (TEM) - JEM 2100 (from Jeol, Japan) was used to observe the morphology of Fe_3O_4-Ag nanohybrids. The dispersion of nanoparticles in the nanocomposite was evaluated by using the scanning electron microscope S-4800 (from Hitachi, Japan) (FE-SEM). To analysize the surface of the coating, a thin carbon layer was applied to increase the electrical conductivity of the coating.

2.3.5. Evaluation of antibacterial activity

Antibacterial tests are similar to those previously published [17], in which, *E. coli* bacteria was inoculated and incubated in 2 ml of LB medium at 37 °C overnight and was shaken at a speed of 200 rpm. After that, the cells were inoculated at 1 % concentration (by v/v cultured cell suspension: LB medium) into 100 ml of fresh LB mediums and these culture mediums are incubated at the above similar condition until their optical density values at λ of 600 nm (OD_{600}) reached about 0.3, the films of 100 mm × 100 mm × 25 µm without (ACUV) containing nanohybrids (ACUV/Fe_3O_4-Ag) are added into incubational tank and keep cultivating. Cultured cell suspensions were determined OD_{600} value after various time of cultivating since adding the films. Each experiment was measured triplicate and the data was presented as average values.

3. Results and discussion

3.1. Crosslinking process of UV curable coating containing Fe_3O_4-Ag nanohybrids

3.1.1. Chemical conversion of acrylate double bonds

IR method was effectively used to investigate the kinetic and mechanism of chemical reaction for both curing reaction and photodegradation of coating [2,3,17,23]. In this work, the kinetic of the curing reaction was monitored IR absorption density of acrylate double bond in the crosslinking reaction of UV-curable coatings. IR spectra of the neat UV-curable acrylate coating (ACUV) and its nanocomposite (ACUV/Fe_3O_4-Ag) before and after 4.8 s of the UV exposue were presented in Fig. 6.

Fg. 6 shows that during the cruring process, the 1634, 1408, 984, 910 and 810 cm^{-1} bands assigning to acrylate double bonds of HDDA and BGDM decreased. Among them, the decrease of the 910 cm^{-1} band was most clearly, so this band was choosed to investigate quantitatively the conversion of acrylate double bonds during the crosslinking process

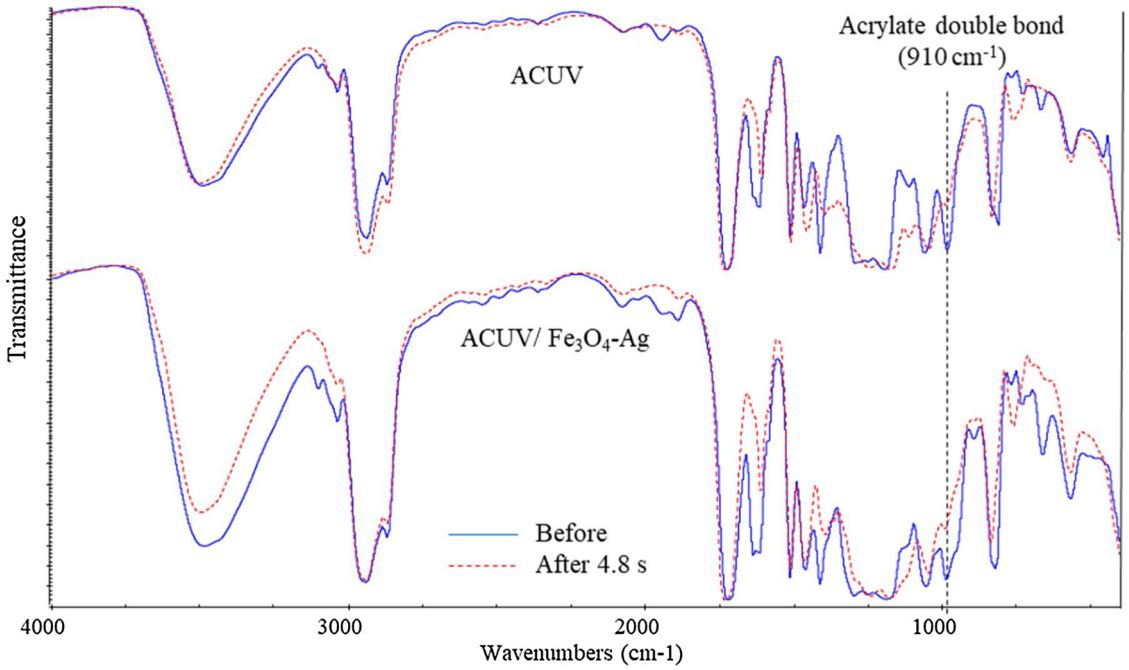

Fig. 6. IR spectra of neat UV curable coating (ACUV) and its nanocomposite (ACUV/Fe_3O_4-Ag) before and after 4.8 s of the UV exposure.

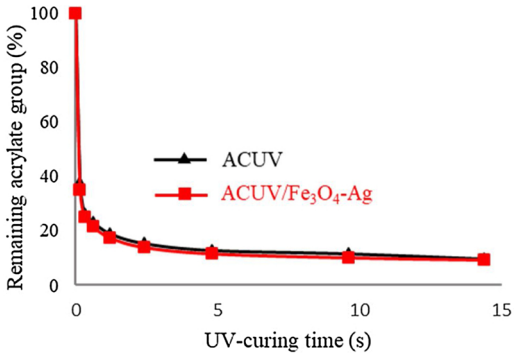

Fig. 7. Conversion of acrylate double bonds during the UV exposure.

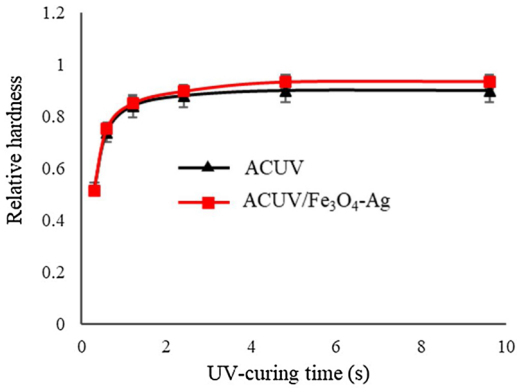

Fig. 8. Modification of relative hardness of the neat coating (ACUV) and the nanocomposite (ACUV/Fe_3O_4-Ag).

of the coatings. The obtained results were shown in Fig. 7.

Fig. 7 shows that the acrylate double bonds quickly converted in the first 0.15 s, after then slowed down. After 4.8 s of the UV exposure, the conversion of the acrylate double bonds seemed to have reached the highest value (87.2 % and 88.3 % for the coating without and with 0.1 wt.% Fe_3O_4-Ag nanohybrids, respectively). The conversion of acrylate double bonds was influenced insignificantly by the presence of the nanohybrids in concentration of 0.1 wt.%.

Photoinitiator was very sensitive to UV radiation [7], under effect of UV radiation of a medium-pressure mercury lamp in FUSION UV equipment, photoinitiator I-184 in high concentration (3 wt.%) was decomposed into free radicals. After then these free radicals reacted with acrylate double bonds and initiated photocrosslinking polymerization reaction while the nanohybrids in low concentration (0.1 wt.%), its absorption of UV is not large enough to affect the UV energy absorption of initiators. This is possible reason for its insignificant influence on the conversion of acrylate double bonds.

3.1.2. Increase of coating hardness

In the crosslinking process, a liquid resin system is converted into a three dimentional network polymer; the coating hardness is thus increased. The modification of the hardness can be linked to its crosslinking degree. Fig. 8 shows the modification of the relative hardness of the neat coating (ACUV) and the nanocomposite (ACUV/Fe_3O_4-Ag). Fig. 8 indicates that the relative hardness rised rapidly after only first 1.2 s of the UV exposure and at a slower rate for later 3.6 s. After 4.8 s, the relative hardness of the coatings reached a highest value of about 0.90 and 0.93 for the coating without and with 0.1 wt% Fe_3O_4-Ag nanohybrids, respectively. The addition of Fe_3O_4-Ag nanohybrids into the polymer matrix increased insignificantly the coating hardness, possibly, because the nanoparticles filled the holes and defects of the coating leading to its tighter structure and its relative hardness was increased, however, in the presence of the nanohybrids, roughness of surface of nanocomposite coating also increased which descreased the relative hardness. These two trends offset each other resulting to the relative hardness increased insignificantly.

3.1.3. Gel and swelling properties of the coatings

Measure the gel fraction and swelling degree of the coatings during photocroslinking process is not only a useful method to study kinetic of crosslinking reaction but also is the way to determine the crosslinking intensity of the coatings. The analysis results of the gel fraction and swelling degree of the coatings were presented in Fig. 9.

As can be seen from Fig. 9 that, after 0.3 s of UV exposure, the gel

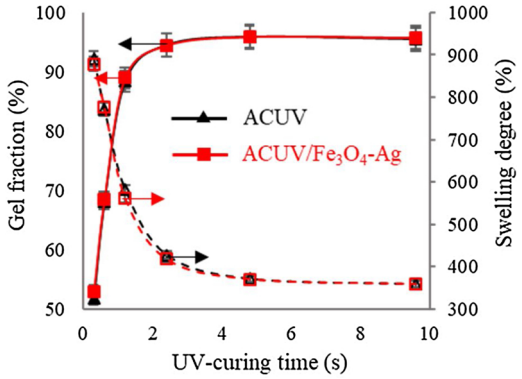

Fig. 9. Variations of gel fraction and swelling degree of the coating without (ACUV) and with Fe_3O_4-Ag nanohybrids (ACUV/Fe_3O_4-Ag).

fraction of the coatings appeared. The gel fraction increased and swelling degree decreased quickly for first 2.4 s. They changed at a slower rate for later 2.4 s. After 4.8 s, the gel fraction reached a maximum value of about 95.8 % and 95.9 % while the swelling degree reached a minimum value of about 371 % and 370 % for the coating without and with 0.1 wt.% Fe_3O_4-Ag nanohybrids, respectively. The presence of Fe_3O_4-Ag nanohybrids in the coating had no effect on its gel fraction and swelling behavior.

3.1.4. Structural morphology of the nanocomposite coating

To observe the structural morphology of the coating, FE-SEM images was performed. The FE-SEM images of UV curing nanocomposite in cross-section were exhibited in Fig. 10

This figure demonstrates that the coating had a tight structure without various defects, cracks. In the nanocomposite, there was no large agglomeration of the nanohybrids. This can be explained that the presence of OA and OLA surfactants leads to a homogeneous dispersion of nanoparticles in the nanocomposite and they are well compatible with polymer matrix. On the base of the data from conversion of acrylate double bonds, variations of relative hardness, gel fraction, swelling degree and structural morphology analysis of the nanocomposite, it could be identified that crosslinking process of UV-curable resin system based on photoinitiator I.184, HDDA, BGDM and Fe_3O_4-Ag nanohybrids was insignificantly influenced by the presence of the nanohybrids as shown in Fig. 11

Thus, Fe_3O_4-Ag nanohybrids and surfactants (OA and OLA) on their surface did not react with components in UV curable system (I.184, HDDA and BGDM). The addition of 0.1 wt.% of nanohybrids possibly increase the UV shielding but not high enough to reduce the reaction rate as well as the conversion of acrylate groups. The UV exposure for the curing completion was calculated to be about 4.8 s.

3.2. Abrasion resistance of the coatings

Abrasion resistance of the neat coating (ACUV) and the nanocomposite (ACUV/Fe_3O_4-Ag) after 4.8 s of the UV exposure was evaluated and shown in Fig. 12.

As can be seen from Fig. 12 that due to the incorporation of the Fe_3O_4-Ag nanohybrids into network polymer, the abrasion resistance of the coating increased from 98.4–126.5 lite/mil (28.8 %). This can be explained by a tight structure without holes and defects of the nanocomposite which had been found in above FE-SEM analysis (Fig. 10).

3.3. Evaluation of antibacterial activity

Effect of the Fe_3O_4-Ag nanohybrids on the antibacterial ability of the nanocomposites on the base of natural rubber–polyethylene blends and acrylic polyurethane coating was reported in our previous works [16,17]. High bactericidal activity of Fe_3O_4-Ag nanohybrids was explained by strong catalytic ability of nano Ag and their good dispersion and aggregation stability due to combinating with the Fe_3O_4 carrier and by a large contact surface between the nanohybrids and bacterial cells. In this work, antibacterial activity of the UV-curable acrylate nanocomposite coatings with difference crosslinking density was investigated. The obtained results of antibacterial tests against *E. coli* were presented in Fig. 13 and Table 1.

The figure demonstrates that the growth rates of the cultures without coating (pure) and with the neat films (ACUV) were insignificantly different. This means that the ACUV film had not antibacterial activity. In the case of the cultures on the nanocomposite films (ACUV/Fe_3O_4-Ag), their growth rates were reduced about 3–5% compared to those in the neat system, after 5 h of cultivation. Fig. 13 and Table 1 indicate that the antimicrobial activity was proportional to the swelling degree of the coating, in other words, it was inversely proportional to its crosslinking intensity. ACUV/Fe_3O_4-Ag film after 4.8 s of curing have a weaker antibacterial activity than that ACPU/Fe_3O_4-Ag film [17]. This could be explained by the fact that the coating with higher crosslinking intensity had tighter structure so the release of Ag^+ ions was more difficult.

4. Conclusion

The kinetic of the UV-curing reaction, morphology, mechanical and antibacterial properties of the nanocomposite based on acrylate resin and Fe_3O_4-Ag nanohybrids as well as influence of crosslinking density of the coating on its antimicrobial activity was studited. The obtained results show that the addition of 0.1 wt.% of Fe_3O_4-Ag nanohybrids into the coating did not influence on its crosslinking process. The UV

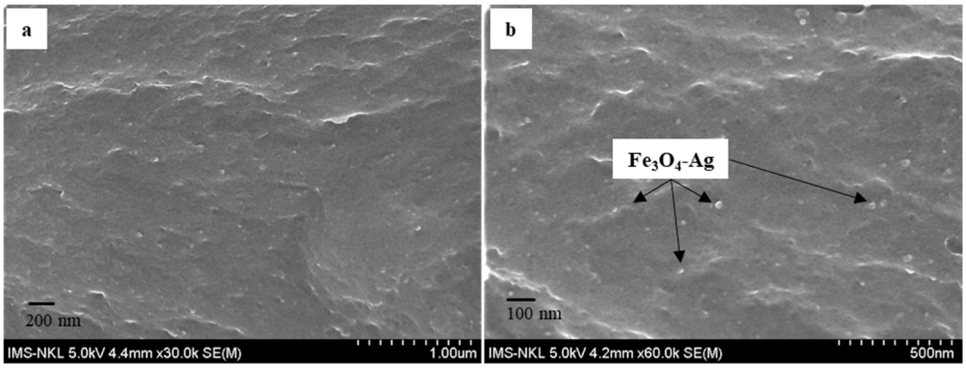

Fig. 10. The FE-SEM images of UV curing nanocomposite (ACUV/Fe_3O_4-Ag) in cross-section at different magnifications: (a) ×30,000 and (b) × 60,000.

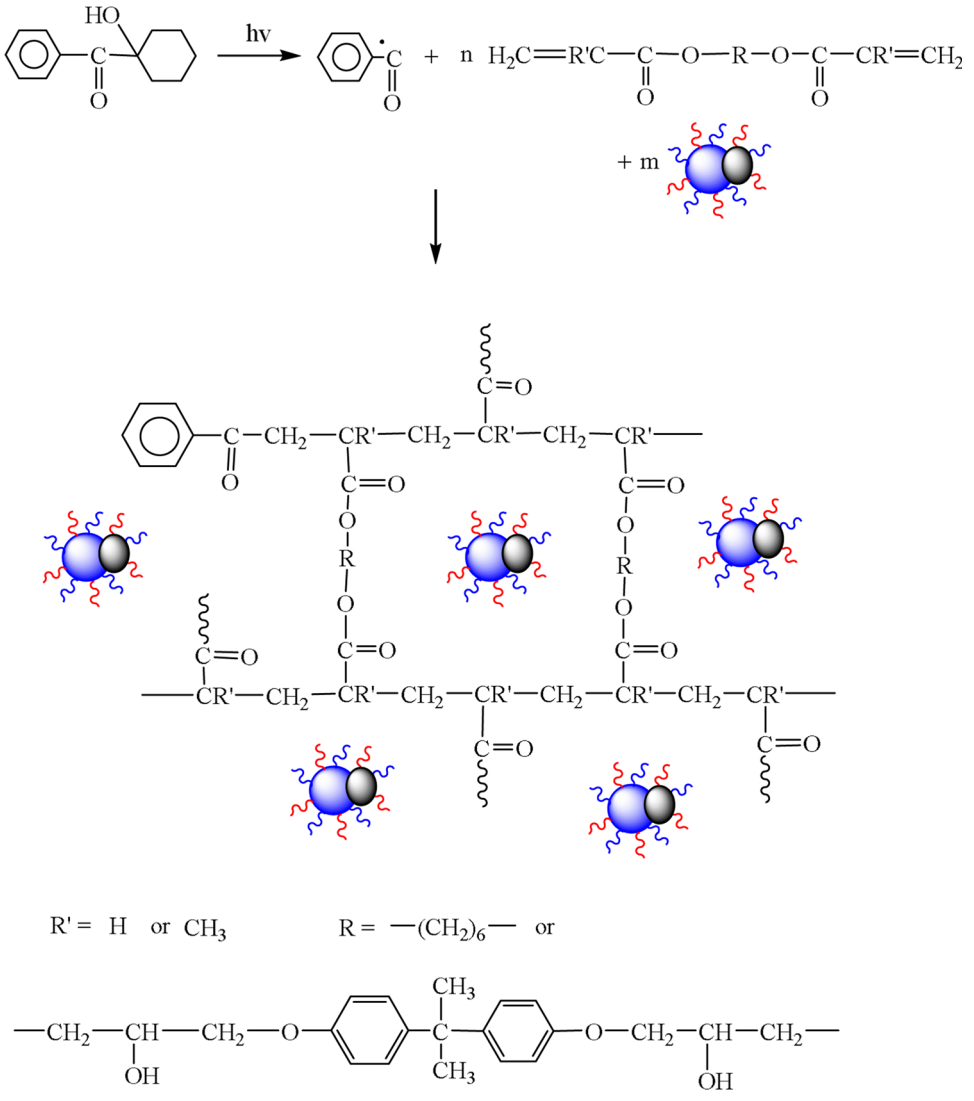

Fig. 11. Crosslinking process of UV-curable resin system based on photoinitiator I.184, HDDA, BGDM and Fe_3O_4-Ag nanohybrids.

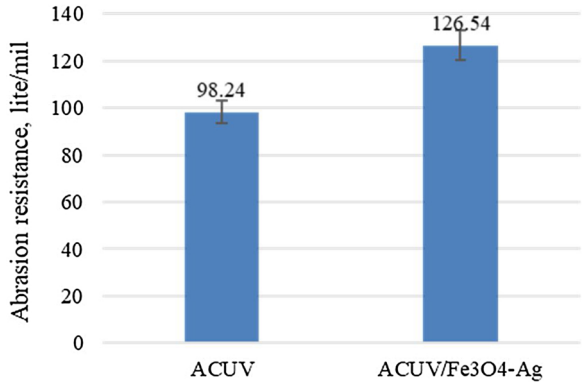

Fig. 12. Abration resistance of the neat coating (ACUV) and the nanocomposite (ACUV/Fe_3O_4-Ag) after 4.8 s of the UV exposure.

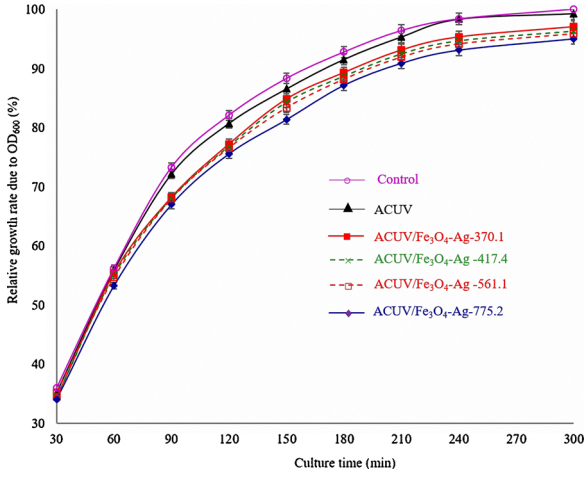

Fig. 13. Influence of the nanocomposites on the growth rate of the cultures.

exposure time to achieve a full crosslinked coating was about 4.8 s with improvement of mechanical properties. Its abrasion resistance rised from 98.24–126.54 lite/mil with the addition of nanoparticles. The antimicrobial activity of the nanocomposite was inversely proportional to the crosslinking density. The growth rates of the cultures containing the nanocomposite reduced about 3–5% compared to those ofin the neat system, after 5 h of cultivation. This antimicrobial nanocomposite with antibacterial agent is promising materials for future smart coatings which can be used as auto-bacteria cleaning surface for various substrates and furnitures.

Table 1
Effect of swelling degree on antibacterial activity of nanocomposite coatings.

No	Coating samples	UV Curing time, s	Swelling degree, %	Growth rate of the cultures after 5 h, %	Name of the cultures
1	ACUV/Fe_3O_4-Ag	0.6	775.2 ± 15	95.04 ± 1	ACUV/Fe_3O_4-Ag-775.2
2		1.2	561.1 ± 11	95.84 ± 1	ACUV/Fe_3O_4-Ag-561.1
3		2.4	417.45 ± 9	94.64 ± 1	ACUV/Fe_3O_4-Ag-417.45
4		4.8	370.3 ± 7.5	97.08 ± 1	ACUV/Fe_3O_4-Ag-370.3
5	ACPU/Fe_3O_4-Ag [17]	6 days	790 ± 15	95.06 ± 1	ACPU/Fe_3O_4-Ag

Acknowledgment

This work was financially supported by the Vietnam National Foundation for Science and Technology Development (NAFOSTED, Grant # 104.02-2018.19).

References

[1] Phuong Nguyen-Tri, Hai Nguyen Tran, Claudiane Ouellet Plamondon, Ludovic Tuduri, Dai-Viet N. Vo, Sonil Nanda, Mishra Abhilasha, Huan-Ping Chao, A.K. Bajpai, Recent progress in the preparation, properties and applications of superhydrophobic nano-based coatings and surfaces: a review, Prog. Org. Coat. 132 (2019) 235–256.
[2] T.V. Nguyen, T.P. Nguyen, T.D. Nguyen, R. Aidani, V.T. Trinh, C. Decker, Accelerated degradation of water borne acrylic nanocomposites used outdoor protective coatings, Polym. Degrad. Stab. 128 (2016) 65–76.
[3] T.V. Nguyen, P.H. Dao, K.L. Duong, Q.H. Duong, Q.T. Vu, A.H. Nguyen, V.P. Mac, T.L. Le, Effect of R-TiO_2 and ZnO nanoparticles on the UV-shielding efficiency of water-borne acrylic coating, Prog. Org. Coat. 110 (2017) 114–121.
[4] H. Salmi, X. Allonas, C. Ley, Polythiourethane networks catalyzed by photobase generators, Prog. Org. Coat. 100 (2016) 81–85.
[5] Federico Magnoni, Agnès Rannée, Liza Marasinghe, Bandar El-Fouhaili, Xavier Allonas, Céline Croutxé-Barghorn, Correlation between the scratch resistance of UV-cured PUA-based coatings and the structure and functionality of reactive diluents, Prog. Org. Coat. 124 (2018) 193–199.
[6] Ehsan Bakhshandeh, Saeed Bastani, Mohammad Reza Saeb, Céline Croutxé-Barghorn, Xavier Allonas, High-performance water-based UV-curable soft systems with variable chain architecture for advanced coating applications, Prog. Org. Coat. 130 (2019) 99–113.
[7] Phuong Nguyen-Tri, Thien Vuong Nguyen, Radically curable nanobased coatings (chapter 10), in: Phuong Nguyen Tri, Sami Rtimi, Claudiane Ouellet-Plamondon (Eds.), Nanomaterials Based Coatings, Elsevier, 2019, pp. 1–35, , https://doi.org/10.1016/B978-0-12-815884-5.00010-7 ISBN: B978-0-12-815884-5.00001-6.
[8] T.V. Nguyen, T.A. Nguyen, P.H. Dao, V.P. Mac, A.H. Nguyen, M.T. Do, T.H. Nguyen, Effect of rutile titania dioxide nanoparticles on the mechanical property, thermal stability, weathering resistance and antibacterial property of styrene acrylic polyurethane coating, Adv. Nat. Sci. Nanosci. Nanotechnol. 7 (4) (2016) 045015–045024.
[9] A.M. El Saeed, M.A. El-Fattah, A.M. Azzam, Synthesis of ZnO nanoparticles and studying its influence on the antimicrobial, anticorrosion and mechanical behavior of polyurethane composite for surface coating, Dye. Pigment. 121 (2015) 282–289.
[10] Hossein Barani, Preparation of antibacterial coating based on in situ synthesis of ZnO/SiO_2 hybrid nanocomposite on cotton fabric, Appl. Surf. Sci. 320 (2014) 429–434.
[11] M. Akbarian, M.E. Olya, M. Ataeefard, M. Mahdavian, The influence of nanosilver on thermal and antibacterial properties of a 2 K waterborne polyurethane coating, Prog. Org. Coat. 75 (4) (2012) 344–348.
[12] R.D. Toker, N. Kayaman-Apohan, M.V. Kahraman, UV-curable nano-silver containing polyurethane based organic–inorganic hybrid coatings, Prog. Org. Coat. 76 (9) (2013) 1243–1250.
[13] The Tam Le, Thien Vuong Nguyen, Tuan Anh Nguyen, ThiThanh Huong Nguyen, Thai Hoang, Dai Lam Tran, Duc Anh Dinh, Thi Mai Nguyen, Le Trong Lu, Thermal, mechanical and antibacterial properties of water-based acrylic polymer/SiO_2-Ag nanocomposite coating, J. Mater. Chem. Phys. 232 (2019) 362–366.
[14] R.K. Kunkalekar, M.M. Naik, S.K. Dubey, A.V. Salker, Antibacterial activity of silver-doped manganese dioxide nanoparticles on multidrug-resistant bacteria, J. Chem. Technol. Biotechnol. 88 (2013) 873–877, https://doi.org/10.1002/jctb.3915.
[15] Phuong Nguyen Tri, Tuan Anh Nguyen, The Huu Nguyen, Pascal Carriere, Antibacterial behavior of hybrid nanoparticles (chapter 7), in: Satyabrata Mohapatra, Tuan Anh Nguyen, Phuong Nguyen-Tri (Eds.), Noble Metal-Metal Oxide Hybrid Nanoparticles: Fundamentals and Applications, 2019, pp. 141–155, , https://doi.org/10.1016/B978-0-12-814134-2.00007-3.
[16] T.D. Ngo, T.M.H. Le, T.H. Nguyen, T.V. Nguyen, T.A. Nguyen, T.L. Le, T.T. Nguyen, T.T.V. Tran, T.B.T. Le, Antibacterial nanocomposites based on Fe_3O_4-Ag hybrid nanoparticles and natural rubber–polyethylene blends, Int. J. Polym. Sci. 2016 (2016) 74781619 pages.
[17] ThiNgoc Linh Nguyen, Truc Vy Do, Thien Vuong Nguyen, Dao Phi Hung, Van ThanhTrinh, Van Phuc Mac, Anh Hiep Nguyen, Duc Anh Dinh, Tuan Anh Nguyen, Thi Kieu Anh Vo, Dai Lam Tran, Trong Lu Le, Antimicrobial activity of acrylic polyurethane/Fe_3O_4-Ag nanocomposite coating, Prog. Org. Coat. 132 (2019) 15–20.
[18] Ki-Ho Nam, Kwangwon Seo, Jongchul Seo, Sher Bahadar Khan, Haksoo Han, Ultraviolet-curable polyurethane acrylate nanocomposite coatings based on surface-modified calcium carbonate, Prog. Org. Coat. (85) (2015) 22–30.
[19] Carola Esposito Corcione, Chiara Ingrosso, Francesca Petronella, Roberto Comparelli, M. Lucia Curri, A designed UV–vis light curable coating nanocomposite based on colloidal TiO2 NRs in a hybrid resin for stone protection, Prog. Org. Coat. 122 (2018) 290–301.
[20] Derya Işın, Nilhan Kayaman-Apohan, Atilla Güngör, Preparation and characterization of UV-curable epoxy/silica nanocomposite coatings, Prog. Org. Coat. 65 (4) (2009) 477–483.
[21] Shengwen Zhang, Aixia Yu, Xiaoqing Song, Xiaoya Liu, Synthesis and characterization of waterborne UV-curable polyurethane nanocomposites based on the macromonomer surface modification of colloidal silica, Prog. Org. Coat. 76 (7–8) (2013) 1032–1039.
[22] Vanessa Maurin, Céline Croutxé-Barghorn, Xavier Allonas, Jocelyne Brendlé, Julia Bessières, André Merlin, Eric Masson, UV powder coatings containing synthetic Ag-beidellite for antibacterial properties, Appl. Clay Sci. 96 (2014) 73–80.
[23] T.V. Nguyen, X.H. Le, P.H. Dao, C. Decker, T.P. Nguyen, Stability of acrylic polyurethane coatings under accelerated aging tests and natural outdoor exposure: the critical role of the used photo-stabilizers, Prog. Org. Coat. 124 (2018) 137–146.
[24] N. Huong, Improvement of Bearing Strength of Laminated Composites by Nanoclay and Z-pin Reinforcement, PhD. Dissertation, University of New South Wales, Australia, 2006.
[25] O. Becker, R. Varley, G. Simon, Morphology, thermal relaxations and mechanical properties of layered silicate nanocomposites based upon high-functionality epoxy resins, Polymer 43 (16) (2002) 4365–4373.
[26] Maryam Jouyandeh, Meisam Shabanian, Mahroo Khaleghi, Seyed Mohammad RezaParan, Samira Ghiyasi, Henri Vahabi, Krzysztof Formela, Debora Puglia, Mohammad Reza Saeb, Acid-aided epoxy-amine curing reaction as reflected in epoxy/Fe_3O_4 nanocomposites: chemistry, mechanism, and fracture behavior, Prog. Org. Coat. 125 (2018) 384–392.
[27] Maryam Jouyandeh, Seyed Mohammad Reza Paran, Meisam Shabanian, Samira Ghiyasi, Henri Vahabi, Michael Badawi, Krzysztof Formela, Debora Puglia, Mohammad Reza Saeb, Curing behavior of epoxy/Fe_3O_4 nanocomposites: a comparison between the effects of bare Fe_3O_4, Fe_3O_4/SiO_2/chitosan and Fe_3O_4/SiO_2/chitosan/imide/phenylalanine-modified nanofillers, Prog. Org. Coat. 123 (2018) 10–19.
[28] Mohammad Reza Saeb, Milad Nonahal, Hadi Rastin, Meisam Shabanian, Mehdi Ghaffari, Ghasem Bahlakeh, Samira Ghiyasi, Hossein Ali Khonakdar, Vahabodin Goodarzi, P. Poornima Vijayan, Debora Puglia, Calorimetric analysis and molecular dynamics simulation of cure kinetics of epoxy/chitosan-modified Fe_3O_4 nanocomposites, Prog. Org. Coat. 112 (2017) 176–186.
[29] Mohammad Reza Saeb, Hadi Rastin, Meisam Shabanian, Mehdi Ghaffari, Ghasem Bahlakeh, Cure kinetics of epoxy/β-cyclodextrin-functionalized Fe_3O_4 nanocomposites: experimental analysis, mathematical modeling, and molecular dynamics simulation, Prog. Org. Coat. 110 (2017) 172–181.
[30] Maryam Jouyandeh, Negar Rahmati, Elnaz Movahedifar, Behzad Shirkavand Hadavand, Zohre Karami, Mehdi Ghaffari, Peyman Taheri, Ehsan Bakhshandeh, Henri Vahabi, Mohammad Reza Ganjali, Krzysztof Formela, Mohammad Reza Saeb, Properties of nano-Fe_3O_4 incorporated epoxy coatings from Cure Index perspective, Prog. Org. Coat. 133 (2019) 220–228.
[31] Liza Marasinghe, Céline Croutxé-Barghorn, Xavier Allonas, Adrien Criqui, Effect of reactive monomers on polymer structure and abrasion resistance of UV cured thin films, Prog. Org. Coat. 118 (2018) 22–29.
[32] Junyi Zhou, Xavier Allonas, Xiaoxuan Liu, Fluorinated organozirconiums: enhancement of overcoming oxygen inhibition in the UV-curing film, Prog. Org. Coat. 120 (2018) 228–233.
[33] Thien Vuong Nguyen, Phuong Nguyen -Tri, Sohrab Azizi, Tran Chien Dang, Duc Minh Hoang, Thu Ha Hoang, Thi Linh Nguyen, Thuy Thi Le Bui, Xuan Thang Dam, Ngọc Linh Nguyen, The Tam Le, ThiNgoc Linh Nguyen, Quoc Trung Vu, Dai Lam Trana, Duc Anh Dinh, Le Trong Lu, The role of organic and inorganic UV-absorbents on photopolymerization and mechanical properties of acrylate-urethane coating, J. Mater. Today Commun. (2019) Under review.
[34] T.L. Le, T.D. Ngo, D.T. Le, T.T. Cao, K.Q. Ong, V.C. Nguyen, M. Shinya, T.K.T. Nguyen, Synthesis of magnetic cobalt ferrite nanoparticles with controlled morphology, monodispersity and composition: the influence of solvent, surfactant, reductant and synthetic conditions, Nanoscale 7 (2015) 19596–19610.